Non-Gaussian behavior of low-order moments in fully developed turbulence

Samuel I. Vainshtein
Department of Astronomy and Astrophysics, University of Chicago, Chicago, Illinois 60637
(Received 21 November 1996)

An experimental study is made of velocity increment statistics in turbulent pipe flow. Special attention is given to positive and negative parts of the increments, corresponding to low-order-moment statistics. In particular, we study the zeroth moment of both positive and negative parts of the distribution, i.e., the box counting for each part separately: that makes it possible to calculate the Kolmogorov capacity. Low-order-moment statistics corresponds to low and moderate velocity increments, which are described by a probability density-function for, say, less than three standard deviations. The distributions prove to deviate noticeable from Gaussian or from some other simple distribution. This implies a deviation from scaling law for the structure functions, suggested by the Kolmogorov hypotheses. [S1063-651X(97)01107-0]

PACS number(s): 47.27.Ak, 47.27.Jv

I. INTRODUCTION

Statistical properties of turbulence have been studied for a long time. In particular, Kolmogorov suggested a scaling law for structure functions, and that is now called K41 theory [1]. As it was understood later, the theory is valid for relatively simple statistics. Roughly speaking, the predicted scaling corresponds to a nonintermittent system, i.e., the probability distributions do not deviate strongly from the Gaussian distribution.

On the other hand, intermittency of turbulence does correspond to a deviation from the Gaussian distribution. Indeed, the refined Kolmogorov hypotheses [2] suggest that the probability distribution differs from the Gaussian one. Strictly speaking, the Kolmogorov law [3], found in 1941, implies that the probability distribution function (PDF) is asymmetric and therefore cannot be Gaussian. However, this deviation has been considered to be small.

Naturally, the deviation from Gaussian statistics manifests itself mainly in high moments. Indeed, many studies (see, e.g., [4,5]) show that if there is an anomalous scaling for the structure functions, then it would be found in the high moments. The same is true for the generalized dimensions D_q corresponding to qth moments. Experimental data persistently showed that the dimensions are trivial for the low moments; for instance, the Kolmogorov capacity $D_0=1$ (if dealing with a one-dimensional cut of a process) and the deviation from unity appears only in higher moments.

Recent studies, however, suggest that the deviation can already be found in the low moments [6]. This is especially true if one considers positive and negative parts of the velocity increments separately. They reveal an *asymmetry* of statistics. As the high moments usually have poor convergence and they can be trusted, say, up to the sixth moment only [7], it appears that the study of low moments statistics could prove to be useful. Low-order-moment-statistics corresponds to the PDF, constructed for low and moderate velocity increments, and therefore the study of this kind of PDF provides supplemental information about the deviation from the Gaussian process.

The rest of the paper is organized as follows. We describe in Sec. II what the Gaussian distribution would predict for the statistics of positive and negative parts of the velocity increments and for low-order statistics. A comparison of these predictions with experimental structure functions of zeroth order is given in Sec. III. Section IV deals with box counting, or the Kolmogorov capacity, of positive and negative parts of the velocity increments. Asymmetry proves to be an obstacle for the construction of a PDF with all the needed properties. For example, in Sec. V an attempt is made to construct a Gaussian-like PDF; this proves to be impossible, at least for the simplest case. Probability distributions for relatively low velocity increments, i.e., below three standard deviations, are presented in Sec. VI. Finally, the main conclusions are given in Sec. VII.

II. MULTIVARIATE GAUSSIAN DISTRIBUTION

We will use the two-point Gaussian distribution, the probability density for the velocity to assume the values v and v', at the points x and x',

$$P_2(v,v'|x,x') = \frac{1}{d_2}\exp\left\{-\frac{K(0)v^2-2K(r)vv'+K(0)v'^2}{2[K(0)^2-K(r)^2]}\right\}, \quad (1)$$

where $K(r)$ is an arbitrary velocity correlation function, $r=x'-x$, and $d_2=2\pi[K(0)^2-K(r)^2]^{1/2}$. For an n-point PDF,

$$P_n(v_1,v_2,\ldots|x_1,x_2,\ldots) = \frac{1}{d_n}\exp\left\{-\sum_{i\neq j}^{n}\frac{K(0)v_i^2-2K(r_{ij})v_iv_j+K(0)v_j^2}{2[K(0)^2-K(r_{ij})^2]}\right\},$$

where d_n is a normalization constant and r_{ij} is the distance between the ith and jth points.

We write Eq. (1) in a different form, which more appropriate for calculating the structure functions:

$$P_2(v,v'|x,x')=\frac{1}{d_2}\exp\left\{-\frac{u^2}{2\sigma(r)^2}-\frac{(v'+u/2)^2}{2[K(0)-\sigma(r)^2/4]}\right\}, \tag{2}$$

where $u=v-v'$ and $\sigma(r)^2=2[K(0)-K(r)]$. The prefactor can be expressed through $\sigma(r)$ as well, $d_2=2\pi\sigma(r)[K(0)\sigma(r)^2/4]^{1/2}$.

The structure functions are defined as integer moments of the velocity increments,

$$\hat{S}_n(r)=\langle[v(x+r)-v(x)]^n\rangle=\langle\Delta v_r^n\rangle. \tag{3}$$

Therefore, integrating Eq. (2) over all v', we get the PDF for u, i.e., for the increments,

$$P(u|x,x')=\frac{1}{\sqrt{2\pi}\sigma(r)}\,e^{-u^2/2\sigma(r)^2}. \tag{4}$$

Obviously, the odd moments vanish, $\hat{S}_n(r)=0$, $n=2m+1$, m is an integer, and

$$\hat{S}_n(r)=G(n)\sigma(r)^n, \tag{5}$$

where $n=2m$ and $G(n)$ is Gaussian constant. In particular, $G(2m)=(2m-1)!!=1\times3\cdots(2m-1)$.

More often, however, the so-called generalized structure functions are used,

$$S_q(r)=\langle|v(x+r)-v(x)|^q\rangle, \tag{6}$$

for arbitrary q. Then, using Eq. (4), for the Gaussian process,

$$S_q(r)=G(q)\sigma(r)^q. \tag{7}$$

If, in addition, all structure functions exhibit scaling properties, an assumption we are making in this paper, then the generalized structure functions would behave like

$$S_q(r)\sim r^{\zeta_q}, \tag{8}$$

which corresponds to the assumption that $\sigma(r)$ should scale like

$$\sigma(r)\sim r^p.$$

Under these assumptions, the Kolmogorov hypotheses can be recovered for the generalized structure functions. Indeed, using Eq. (7),

$$\zeta_q=qp. \tag{9}$$

There are two ways of finding p. One is to consider dimensional arguments, that is, to write the only dimensional combination, as in [1],

$$\langle|\Delta v_r|\rangle=S_1(r)\sim(\epsilon r)^{1/3}, \tag{10}$$

where ϵ is the energy dissipation rate. In that case, $p=\frac{1}{3}$. Another way, with the same result, is to notice the *experimental* closeness of the exponents for $S_3(r)$ and $\hat{S}_3(r)$ [8] and to invoke the $\frac{4}{5}$ Kolmogorov law [3],

$$\hat{S}_3(r)=-\tfrac{4}{5}\epsilon r. \tag{11}$$

It follows that $\zeta_3=1$ and $p=\frac{1}{3}$ from (9).

This scaling indeed corresponds to the Kolmogorov hypotheses K41 [1],

$$S_q(r)\sim(\epsilon r)^{q/3}, \tag{12}$$

although they are usually written for the structure functions rather than for generalized structure functions, namely,

$$\hat{S}_n(r)\sim r^{\xi_n},$$

where

$$\xi_n=\frac{n}{3}. \tag{13}$$

As the structure functions coincide with the general structure functions for even (integer) q, we simply have $\zeta_{2m}=\xi_{2m}$. In addition, the expression for the structure function, with exponents like Eq. (13), can be roughly used for the odd moments as well [except, of course, for $q=1$, because $\langle v(x+r)-v(x)\rangle=0$]. The point here is that Eq. (13) is satisfied for $q=3$ because of the Kolmogorov law and, according to experimental data [8,4(d)], the higher-order odd exponents also roughly obey the Kolmogorov hypotheses (13).

The mere existence of the Kolmogorov law (11) and nonvanishing odd moments means that the PDF is not Gaussian, but is asymmetric. We will be able to make more quantitative statements by studying positive and negative parts of velocity increments. Namely, we consider, following [9],

$$S_q^{\pm}(r)=\langle\{\tfrac{1}{2}[|\Delta v_r(x)|\pm\Delta v_r(x)]\}^q\rangle. \tag{14}$$

Obviously, $[|\Delta v_r(x)|\pm\Delta v_r(x)]/2$ are non-negative and represent positive parts of $\Delta v_r(x)$ for the plus and the absolute value of negative parts for the minus.

One of the quantities that measures the deviation from Gaussian process is the flatness factor

$$F_4(r)=\frac{S_4(r)}{S_2(r)^2}. \tag{15}$$

For the Gaussian process, F_4 is independent of r and equal to $G(4)/G(2)^2=3$, by Eq. (7). Obviously, in that case, $S_2(r)^{\pm}=S_2(r)/2$, $S_4(r)^{\pm}=S_4(r)/2$, and therefore

$$F_4^{\pm}=\frac{S_4^{\pm}(r)}{[S_2^{\pm}(r)]^2}=6. \tag{16}$$

Much attention will be devoted to extremely low q, in particular, $q=0$. It easy to see from Eq. (4) that

$$S_0^{\pm}(0)=0,\quad S_0^{\pm}(r\neq0)=\frac{1}{2} \tag{17}$$

for the Gaussian process. Note that the theoretical values of $S_0(r)$ are

$$S_0(0)=0,\quad S_0(r>0)=1, \tag{18}$$

which are valid not only for the Gaussian process, but for any PDF, unless it contains $\delta(\Delta v_r)$.

The two distributions

$$\Delta^+(x)=\tfrac{1}{2}[|\Delta v_{r_0}(x)|+\Delta v_{r_0}(x)]$$

and

$$\Delta^-(x)=\tfrac{1}{2}[|\Delta v_{r_0}(x)|-\Delta v_{r_0}(x)]$$

deserve special attention. Here r_0 corresponds to the smallest separation between two data points in any particular experiment. The distributions correspond to the derivative $\omega(x)=\partial_x v(x)$ or to the positive and negative parts of velocity gradient distribution. To be more specific, $\omega(x)=\Delta^+(x)-\Delta^-(x)$ and $|\omega(x)|=\Delta^+(x)+\Delta^-(x)$. As the sets of nonzero values of $\Delta^+(x)$ and $\Delta^-(x)$ do not intersect, all moments are constructed via the moments of $\Delta^+(x)$ and $\Delta^-(x)$ distributions. For example, the generalized dimensions D_q are obtained from the expression

$$B_q(r)=\langle\omega(r)^q\rangle\sim r^{-(1-D_q)(q-1)}\sim C_q^+ r^{-(1-D_q^+)(q-1)}+C_q^- r^{-(1-D_q^-)(q-1)}, \tag{19}$$

where the angular brackets denote the global average over the local mean,

$$\langle\omega(r)^q\rangle=\frac{\sum_i \omega_i(r)^q}{N},$$

$$\omega_i(r)=\frac{1}{r}\int_{x_i}^{x_i+r}|\partial_x v(x)|dx.$$

Here $N=1/r$ is the number of boxes of size r into which the volume $V=1$ has been divided [10,11]. On the other hand, $\omega_i(r)=\Delta_i^+(r)+\Delta_i^-(r)$, where

$$\Delta_i^{\pm}(r)=\frac{1}{r}\int_{x_i}^{x_i+r}\Delta(x)^{\pm}dx,$$

and thus expression (19) is recovered [9].

As mentioned in the Introduction, the Kolmogorov capacity $D_0=1$ for turbulent processes. In fact, this is a consequence of the *continuity* of the velocity field, which in turn is provided by a finite viscosity.

The situation is quite different with $\Delta^+(x)$ and $\Delta^-(x)$ distributions. They are discontinuous and therefore might be nontrivial. In addition to that, if $D_0^+<1$ or $D_0^-<1$, then all higher-order dimensions are nontrivial. Indeed, according to the theorem [10], $D_{q>0}\leqslant D_0$. Therefore, the Kolmogorov capacity of plus-minus distributions might contain some deep properties of the asymmetry of turbulence.

Related properties might contain the two-point correlations such as $\langle|\omega(x+r)\omega(x)|^{q/2}\rangle$ [11]. We are interested in lowest moment $q=0$. If $v(x)$ is a Gaussian process then its derivative $\omega(x)$ is Gaussian as well. Then, to calculate these correlations, we use Eq. (1), with the correlation function corresponding to $\omega(x)$, i.e.,

$$K(r)=\langle\omega(x+r)\omega(x)\rangle,$$

rather than to the velocity correlations. In particular, we are interested in constructing $K_q^+(r)=\langle[\Delta^+(x+r)\Delta^+(x)]^{q/2}\rangle$ and $K_q^-(r)=\langle[\Delta^-(x+r)\Delta^-(x)]^{q/2}\rangle$ correlations. For the Gaussian process, we have, for $q=0$,

$$\begin{aligned}K_0^+(r)=K_0^-(r)&=\langle[\Delta^+(x+r)\Delta^+(x)]^0\rangle\\&=\langle[\Delta^-(x+r)\Delta^-(x)]^0\rangle\\&=\int_0^\infty dv'\int_0^\infty dv\ P_2(v,v'|x,x+r)\\&=\int_0^\infty dx\int_z^\infty dy\ \frac{1}{2\pi}\,e^{-(x^2+y^2)/2},\end{aligned} \tag{20}$$

where

$$z=-x\,\frac{K(r)}{[K(0)^2-K(r)^2]^{1/2}}.$$

After quite straightforward calculations, we get

$$\begin{aligned}K_0^+(r)=K_0^-(r)&=\langle[\Delta^-(x+r)\Delta^-(x)]^0\rangle\\&=\frac{1}{4}+\frac{1}{2\pi}\arctan[\alpha(r)],\end{aligned} \tag{21}$$

$$\alpha(r)=\frac{K(r)}{[K(0)^2-K(r)^2]^{1/2}}.$$

For $r=0$, $\alpha\to\infty$ and the correlations (20) reach their maximum value (as they should for any correlation function) equal to $\frac{1}{2}$. For $r\to\infty$, $\alpha\to 0$ and these correlations asymptotically approach $\frac{1}{4}$. Finally, note that $\langle|\omega(x+r)\omega(x)|^0\rangle\equiv 1$ for the Gaussian (and, practically, for any other continuous) distribution.

Return to the definition of generalized dimensions, as in Eq. (19). In particular, we are interested in box counting, which gives a generalized dimension for $q=0$. Consider the box counting for plus-minus distributions separately, namely,

$$B_0^{\pm}(r)=\langle\Delta^{\pm}(r)^0\rangle. \tag{22}$$

It is clear that for the Gaussian process (as, in fact, for any other, with a symmetric PDF),

$$B_0^{\pm}(1)=\tfrac{1}{2}. \tag{23}$$

For $r=r_0=2$, one has to consider the two-point distribution (1). Then

$$B_0^{\pm}(r_0)=1-\int_0^\infty dv'\int_0^\infty dv\ P_2(v,v'|x,x+r_0), \tag{24}$$

and using Eqs. (20) and (21),

$$B_0^{\pm}(r_0)=\frac{3}{4}-\frac{1}{2\pi}\arctan[\alpha(r_0)]. \tag{25}$$

Thus expressions for box counting, if each box contains only two points, are expressed via finite integrals. Generally,

$$B_0^{\pm}(r)=1-\int_0^\infty dv_1\int_0^\infty dv_2\cdots P_n,$$

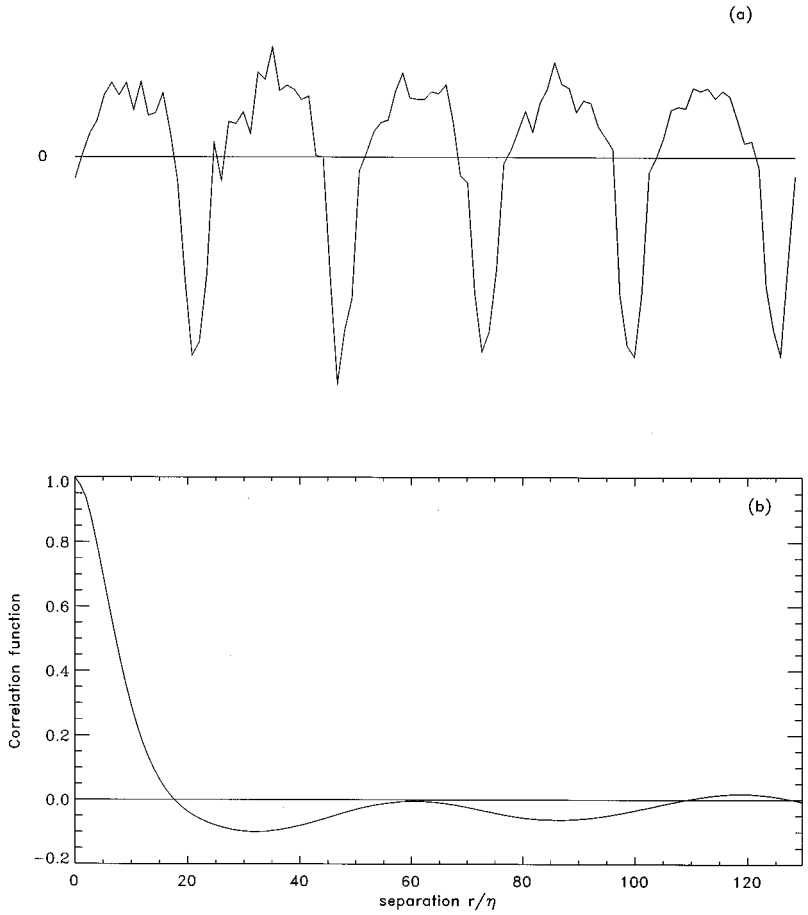

FIG. 1. Illustration of (a) an asymmetric random process; the units are arbitrary, with a correlation function similar to the experimental one, depicted in (b). The latter corresponds to $K(r)=\langle\omega(x+r)\omega(x)\rangle$, where $\omega(x)=\partial_x v(x)$, i.e., the gradient of the measured velocity.

where n is chosen is such a way that $r=r_n$, and r_n is the size of the box. This expression is complicated and therefore not very useful. It is clear from it, though, that for a given P_n, the result of box counting is unambiguously defined; if the process is multivariate Gaussian, then the PDF itself is unambiguously defined by a given correlation function. Therefore, instead of using this complicated expression, we will compare experimental box counting with that of the numerically simulated Gaussian process; the correlation function needed to define the process we take from experiment.

III. MEASUREMENTS OF THE STRUCTURE FUNCTIONS OF ZEROTH ORDER

All measurements reported in this paper were made in a pipe flow of water at a bulk Reynolds number equal to 230 000. The time sequence was treated as a spatial cut by invoking Taylor's hypothesis. The Taylor microscale was estimated to be 0.88 cm and the Kolmogorov microscale was estimated as $\eta=0.27$ mm. All distances in the figures are given in terms of η. A data file with 2×10^6 points was processed.

We start with robust characteristics of the process, namely, experimental measurements of the flatness. For $r=r_0$,

$$F_4(r_0)=5.91, \tag{26}$$

corresponding to moderate intermittency. Now, for the plus-minus distributions we have

$$F_4^+(r_0)=\frac{S_4^+(r_0)}{[S_2(r_0)^+]^2}=9.94 \tag{27}$$

and

$$F_4^-(r_0)=\frac{S_4^-(r_0)}{[S_2(r_0)^-]^2}=12.98. \tag{28}$$

These two values are bigger than the Gaussian one, 6 [Eq. (16)], but the process is not Gaussian already, at least because the regular flatness is higher than 3 [Eq. (26)]. For any symmetric PDF, not necessarily Gaussian, the values of flatness are expected to be $F_4^{\pm}=2F_4(r_0)=11.82$. We see that the plus distribution is less intermittent, i.e., the flatness factor is less than 11.82, and the minus distribution is more intermittent ($F_4^->11.82$). A weak deviation from the symmetry would result in a small deviation of these two numbers from 11.82. The difference $F_4^-(r_0)-F_4^+(r_0)$ is, however, about 26% of the value, which is quite substantial.

Figure 1(a) illustrates a numerical example of such a process. A realization of velocity increments at small lag $v(x+r_0)-v(x)$ or velocity gradient $\omega(x)$ is plotted. The example is constructed in such a way that $\langle\omega\rangle=0$. It is clear that $\langle\omega^3\rangle<0$, i.e., the skewness is negative. It is also obvious that the positive part of ω is less intermittent than the negative one, i.e., the flatness of the negative part is bigger [cf. Eqs. (27) and (28)]. This illustrates the ramp model suggested in [9].

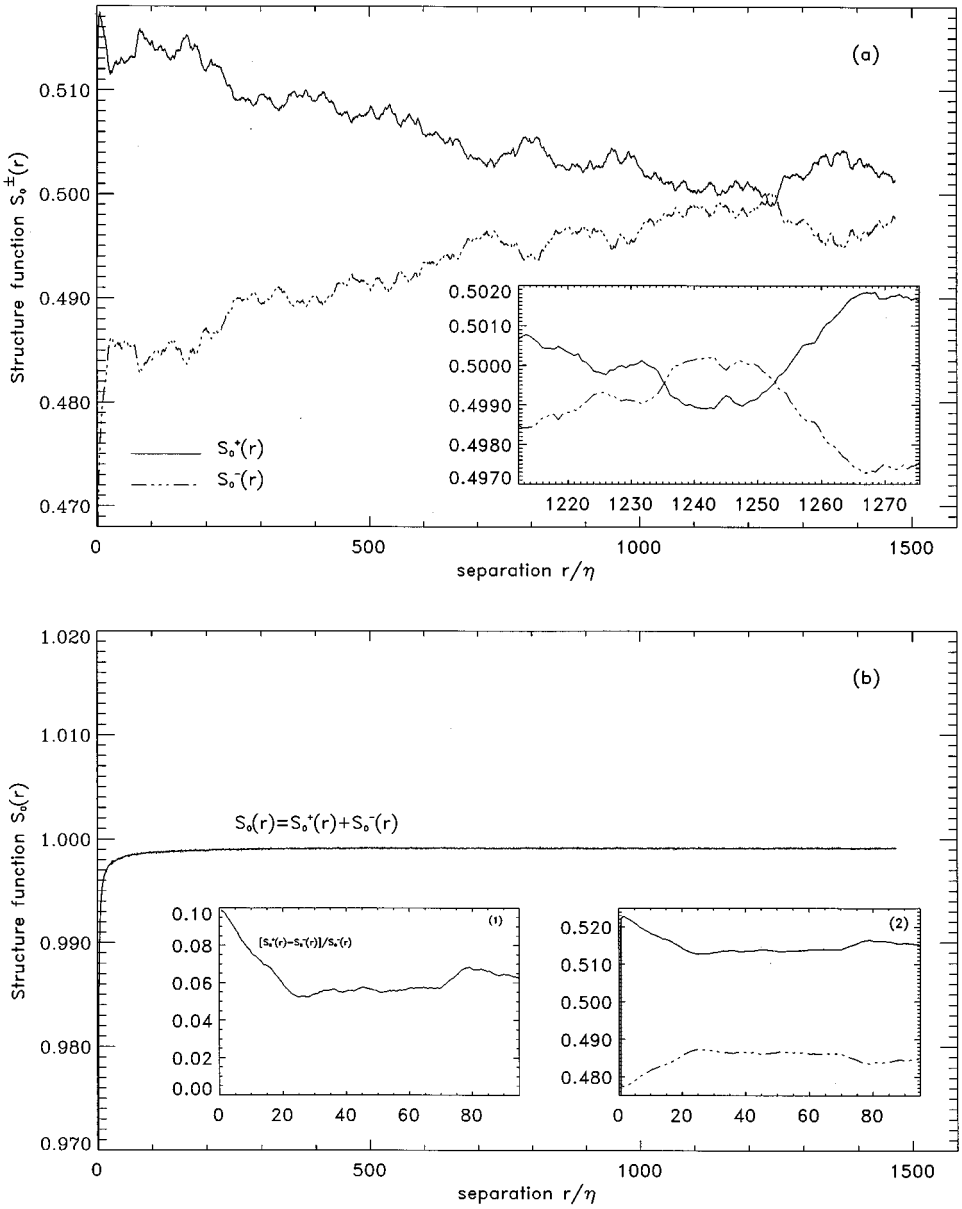

FIG. 2. (a) Plus and minus structure functions of zeroth order. The inset corresponds to the ''anomalous'' region, where the positive length becomes smaller than the negative one. The traditional structure function $S_0(r)$ is given in (b). It looks much smoother. Inset (1) depicts relative asymmetry for small separations and inset (2) shows improved structure functions: the solid line is for $S'^{+}_{0}(r)$ and the dot-dashed line is for $S'^{-}_{0}(r)$.

A correlation function of this process would behave like that in Fig. 1(b), which actually depicts the experimental correlation function of the flow in a pipe. Indeed, the mean square of the deep minima essentially defines the maximum of the correlation function, i.e., $K(0)$. The width of these deep pits defines the correlation length. Finally, positive parts anticorrelate with minima and therefore correspond to the negative part of the correlation function, the extension of it roughly corresponding to the length of the positive parts of the process. Therefore, the correlation function of the numerical example in Fig. 1(a) would have a short correlation length and a wide negative part, i.e., anticorrelation, and the experimental correlation function looks the same.

We note, however, that this comparison is not unambiguous. The point here is that it is possible to construct a pure Gaussian process, with the correlation function like that depicted in Fig. 1(b). In fact, we did construct such a process numerically, and it is used below. We only claim that the ramplike process in Fig. 1(a) would definitely have such a correlation function.

The Kolmogorov law (11) implies that the third moment is negative not only for smallest separation $r=r_0$, but at any scale in inertial range. This implies in turn that the increments $v(x+r)-v(x)$ for a fixed r, not necessarily corresponding to the smallest separation r_0, also look like those depicted in Fig. 1(a). In order to check this, we measured $S_0^{\pm}(r)$ structure functions for bigger r's. Note that the positive parts of this kind of distribution occupy more space than the negative parts, as it can be clearly seen from Fig. 1(a). Obviously, $S_0^{\pm}(r)$ simply represent the relative length of the positive and negative parts or accelerated and decelerated lags of the ramp [9,6]. Figure 2(a) shows these two functions, and indeed the length of the positive parts is bigger than that of the negative ones. Moreover, one can notice the mirror symmetry of these two curves: an increase of the positive length is accompanied by a decrease in the negative lag and vice versa. Even when, as an exception, the positive length becomes smaller than the negative (see the inset), the curves are still mirror symmetric. Of course, if, say, the posi-

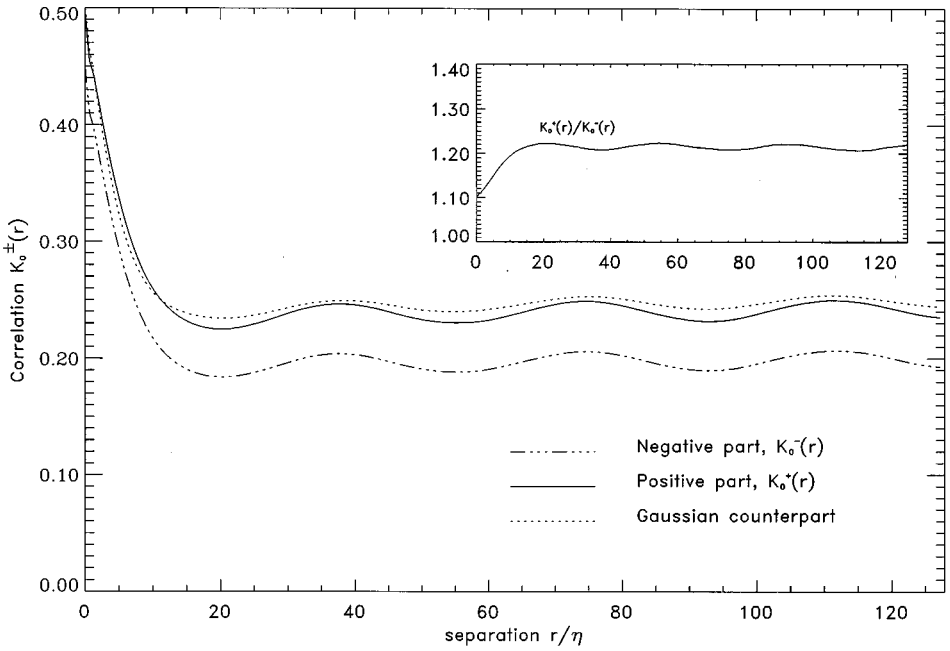

FIG. 3. Zeroth-order correlations $K_0^+(r)$ and $K_0^-(r)$ are plotted and compared with their Gaussian counterparts. The inset gives their ratio.

tive part occupies more space than ''normal,'' then it happens only at the expense of the negative part; therefore, their sum, which is actually the traditional structure function $S_0(r)$, is presented by a much smoother curve, which is depicted in Fig. 2(b) on the same scale range as the two in Fig. 2(a). In contrast, the relative asymmetry $[S_0^+(r) - S_0^-(r)]/S_0^-(r)$ changes dramatically and reaches about 10% at small lags [see inset (1) to Fig. 2(b)].

Another thing that emerges from Fig. 2(b) is that the experimental curve for $S_0(r)$ is slightly below its theoretical value (18). Strictly speaking, the probability for the velocity increment to be exactly zero is zero and hence the theoretical value $S_0(r>0)=1$. Due to the round-up errors, however, the measurements do give some nonzero probability for zeros and therefore $S_0(r>0)\lesssim 1$. Making use of this deviation from unity, we are able to ''improve'' the plus and minus structure functions. Namely, we divide the zeros into two equal parts and attribute each of the parts to the positive and negative distributions. In other words, we introduce improved structure functions $S'^{\pm}_0(r)$,

$$S_0'^{\pm}(0)=0, \quad S_0'^{\pm}(r>0)=S_0^{\pm}(r>0)+\frac{1-S_0(r>0)}{2},$$

so that their sum, that is, the improved structure function $S_0'(r)$, satisfies Eq. (18). The improved structure functions look quite similar to $S_0^{\pm}(r)$, except they are even more mirror symmetric, especially at small distances; see inset (2) in Fig. 2(b).

As suggested in [9] and observed in [6], all negative moments of orders $q>1$ are bigger than the positive moments and vice versa for $q<1$ (they coincide for $q=1$ by definition). Figure 2(a) shows that this rule is quite convincingly confirmed for $q=0$.

IV. ZEROTH-ORDER CORRELATIONS AND BOX COUNTING

We study in this section the two distributions $\Delta^+(x)$ and $\Delta^-(x)$, defined in Sec. II. Experimental zeroth-order correlations $K_0^+(r)$ and $K_0^-(r)$ are depicted in Fig. 3. These are compared with the Gaussian correlation, using Eq. (21). While the plus function is reasonably close to Gaussian, the negative is lower, by approximately 21%; see the inset to the figure. The difference is appreciable. Another thing that emerges from Fig. 3 is that the negative moment is below the positive one, exactly as in Fig. 2(a). That, as pointed out at the end of the preceding section, is to be expected for all moments with $q<1$.

We proceed now to the box counting. Figure 4 shows the box counting for the positive and negative distributions. As mentioned at the end of Sec. II, it is difficult to use the analytical expression for $B_0^{\pm}(r)$ for a Gaussian process because it is very complicated. We generated instead a Gaussian process numerically (with 2^{18} data points), with a correlation function similar to the experimental one. Of course, positive and negative parts practically coincide for this process and are presented as a dotted line in Fig. 4(a). For $r=1$, the box counting simply corresponds to the mean of the number of filled boxes. The Gaussian process naturally results in $B_0^{\pm}(1)=\frac{1}{2}$.

Experimental measurements of $B_0^+(1)$ give a slightly smaller value, while $B_0^-(1)$ is substantially less. Both the positive and negative distributions deviate from the Gaussian distribution. More important is their deviation from each other. The inset shows their ratio reaches 10% above unity. Note that $B_0^+(r)/B_0^-(r)>1$ for all r, i.e., the negative moment is below the positive one, as is to be expected.

In spite of the fact that the deviation from the Gaussian distribution is not that dramatic, we attempted to search for a scaling range, which proved to be for one decade [Fig. 4(b)]. The real incentive for doing this was that, according to Eqs.

(27) and (28), the process is quite intermittent, unlike, of course, the simulated Gaussian process.

The Kolmogorov capacities are then found from expression (19) with $q=0$,

$$B_0^+(r)\sim r^{1-D_0^+}, \quad B_0^-(r)\sim r^{1-D_0^-}, \tag{29}$$

[see also [11], formula (2.9), and [9], formula (14)].

The Kolmogorov capacities calculated for these processes obey the inequality

$$D_q^-<D_q^+, \tag{30}$$

suggested in [9], and the difference between them is within confidence limits; see Fig. 4(b). Furthermore, *if these two curves possess any scaling at all*, this inequality should be satisfied. The point here is that the box counting for any process is a monotonic function, asymptotically approaching unity for big boxes, that is, for $r\to\infty$. Now, as mentioned, the negative counting is always below the positive, so that the negative curve is inevitably steeper than the positive one. As a result, according to Eq. (29), inequality (30) should be satisfied.

V. ATTEMPT TO CONSTRUCT A PSEUDO-GAUSSIAN FUNCTION OR SOME OTHER SIMPLE ASYMMETRIC PDF

The simple expression for the generalized structure functions (7) appears because the multivariate Gaussian distribution depends on only one (functional) parameter $\sigma(r)$. In other words, *any* PDF that can be presented in the form

$$P(u,r)=\frac{1}{\sigma(r)}\,P(y), \quad y=\frac{u}{\sigma(r)} \tag{31}$$

would result in this kind of expression. Indeed, it follows from Eq. (31) that

$$S_q(r)=F(q)\sigma(r)^q, \tag{32}$$

where $F(q)=\int dy|y|^qP(y)$: these are constants, so that the r dependence coincides with Eq. (7) [12].

If we suppose that, generally, $P(y)$ is asymmetric and that $\int dy\ yP(y)=0$, then we recover the Kolmogorov hypotheses (13). Indeed, in that case,

$$\hat{S}_n(r)=\hat{F}(n)\sigma(r)^n, \tag{33}$$

where n is an integer and $\hat{F}(n)=\int dy\ y_nP(y)$. Because of the asymmetry of $P(y)$, the odd moments do not vanish (except for the first order).

It is possible to make an even stronger statement about the velocity increment PDF in the form (31). It is known that any random process can be unambiguously defined either through the moments of arbitrary orders or through its PDF [13]. Thus, *assuming* the PDF in the form (31), we recovered the Kolmogorov hypotheses (12) and (13) using Eqs. (32) and (33). On the other hand, expressions (12) and (13) are valid for any q and therefore *accepting* the Kolmogorov hypotheses, we should be able to recover the velocity increment PDF. Now, knowing that the latter is unambiguously defined by the moments, we are able to claim that Eq. (31) is the only form for the PDF where $\sigma(r)=(\epsilon r)^{1/3}$ using (12).

Thus the PDF in the form (31) does recover the Kolmogorov hypotheses. This simple picture breaks down, however, when we develop it and when trying to fit experimental data, assuming some form of asymmetric $P(y)$. We start, however, with a slightly more complicated PDF, that is, a two-parameter distribution. Namely, let

$$P(u,r)=\frac{a^+}{\sigma(r)^+}\,P^+(y), \quad y=\frac{u}{\sigma(r)^+} \quad \text{for } u\geqslant 0 \tag{34a}$$

and

$$P(u,r)=\frac{a^-}{\sigma(r)^-}\,P^-(y), \quad y=\frac{u}{\sigma(r)^-} \quad \text{for } u<0. \tag{34b}$$

Then, from normalization

$$\int P(u,r)du=1,$$

it follows that

$$F^-(0)a^-+F^+(0)a^+=1, \tag{35}$$

where

$$F^\pm(n)=\int_0^\infty y^nP^\pm(y)dy.$$

Now,

$$\langle\Delta u_r\rangle=\int u\ P(u,r)du=0,$$

that is,

$$F^-(1)a^-\sigma^-(r)=F^+(1)a^+\sigma^+(r). \tag{36}$$

It is clear from Eq. (36) that the two functions $\sigma^+(r)$ and $\sigma^-(r)$ actually coincide, within some coefficient constants. These constants can be included in the normalization coefficients, so that the PDF is not really two parameters.

To keep the PDF as close to the Gaussian form as possible, we suppose that

$$P^-(y)=P^+(y)=\frac{1}{\sqrt{2\pi}}\,e^{-y^2/2}, \tag{37}$$

i.e., both functions are Gaussian, although the argument y is defined differently in the positive and negative regions, using Eq. (34). Then, as $F^+(0)=F^-(0)=G(0)/2=\frac{1}{2}$ for this case, and introducing the asymmetry parameter $s=1-a^+$ (i.e., $a^+=1-s$), we get $a^-=1+s$ and

$$\sigma^-(r)=(1-s)\sigma(r), \quad \sigma^+(r)=(1+s)\sigma(r),$$

using Eq. (36).

We are now in position to calculate the structure functions, namely,

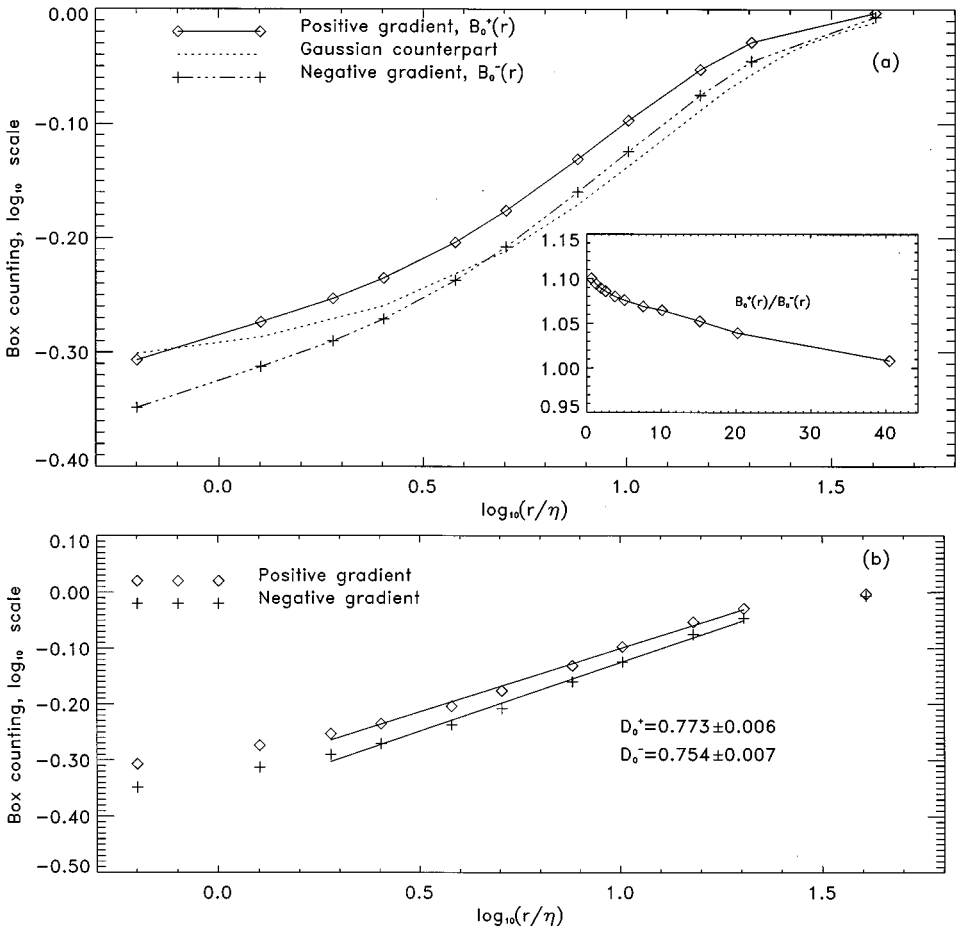

FIG. 4. Box counting for the velocity gradient. (a) Positive $B_0^+(r)$ and negative $B_0^-(r)$ parts of the distribution. For comparison, a numerically simulated Gaussian process, with a correlation function similar to the experimental one, is plotted. The inset gives their ratio. (b) An attempt to find a scaling and the corresponding Kolmogorov capacities.

$$\hat{S}_n(r)=S_n^+ +(-1)^n S_n^-(r) = \frac{G(n)}{2}\,\sigma(r)^n[(1-s)(1+s)^n + (-1)^n(1+s)(1-s)^n] \tag{38}$$

for integer n and

$$S_q(r)=S_q^+ + S_q^-(r) = \frac{G(q)}{2}\,\sigma(r)^q[(1-s)(1+s)^q+(1+s)(1-s)^q] \tag{39}$$

for arbitrary q. As $G(0)=1$, we recover Eq. (18) for $n=q=0$. For $n=1$, Eq. (38) turns to zero, as it should.

For the symmetric distribution, $s=0$ and all odd moments for $\hat{S}_n(r)$ vanish. The asymmetry parameter s is analogous to the skewness, except the former is bounded $-1<s<1$. According to the Kolmogorov law, the third moment is negative, which implies that $s<0$.

Clearly, the Kolmogorov hypotheses, both for $S_q(r)$, with exponents from Eq. (12), and for the structure functions, with exponents from Eq. (13), are recovered by using expressions (38) and (39) if $\sigma(r)\sim r^{1/3}$ in inertial range.

The ratio of plus and minus parts can be obtained from Eq. (38) or (39),

$$\frac{S_q^+(r)}{S_q^-(r)}=\frac{(1-s)(1+s)^q}{(1+s)(1-s)^q}=\left(\frac{1+s}{1-s}\right)^{q-1}. \tag{40}$$

As $s<0$, it follows from Eq. (40) that $S_q^-(r)>S_q^+(r)$ for $q>1$ and $S_q^-(r)<S_q^+(r)$ otherwise. This corresponds to the experimental rule [6], mentioned above. Thus, so far, this asymmetric PDF works.

Furthermore, an expression like Eq. (40) can be obtained not only for a pseudo-Gaussian PDF, as in this case, but for any one-parameter distribution (only with different coefficients those in Eqs. (38) and (39), instead of $G(q)$), provided $P^-(y)=P^+(y)=P(y)$, i.e., the first equality in Eq. (37) is satisfied.

This requirement seems to be quite innocent, but it is not the case; it is at this point where the constructed PDF breaks down. Indeed, according Eqs. (34) and (36), in this case,

$$P(u,r)=\frac{1-s}{(1+s)\sigma(r)}\,P(y),\quad y=\frac{u}{(1+s)\sigma(r)}\quad \text{for } u\geqslant 0, \tag{41a}$$

$$P(u,r)=\frac{1+s}{(1-s)\sigma(r)}\,P(y),\quad y=\frac{u}{(1-s)\sigma(r)}\quad \text{for } u<0, \tag{41b}$$

and there is a jump in the PDF at $u=0$ (i.e., $y=0$), from

$$\frac{1+s}{(1-s)\sigma(r)}\,P(0)$$

to

$$\frac{1-s}{(1+s)\sigma(r)}\,P(0)$$

for *any* separation r. Furthermore, the jump increases for small $\sigma(r)$, i.e., for small separations r, and becomes big for small r's, however weak the asymmetry is (i.e., even for infinitesimal small s). This has not been observed experimentally. In particular, for the data studied in this paper, the PDF is smooth at the origin (see Sec. VI).

The only way to get rid of this discontinuity is to return to the PDF in the strictly one-parameter form (31), with asymmetric $P(y)$. Then, using the previous denotation, the two functions $P^{\pm}(y)$ simply correspond to the positive and negative regions of argument for the function $P(y)$, i.e., $P^{+}(y)=P(y\geqslant 0)$ and $P^{-}(y)=P(y\leqslant 0)$ [so that $P^{+}(0)=P^{-}(0)$].

The normalization results in

$$F^{-}(0)+F^{+}(0)=1, \tag{42}$$

an analog of Eq. (35), and the vanishing first moment leads to the expression

$$F^{-}(1)=F^{+}(1), \tag{43}$$

an analog of (36). As above, we construct the expressions for the structure functions

$$\hat{S}_n(r)=S_n^{+}+(-1)^n S_n^{-}(r)=\sigma(r)^n[F^{+}(n)+(-1)^n F^{-}(n)] \tag{44}$$

for integer n [cf. Eq. (38)] and

$$S_q(r)=S_q^{+}+S_q^{-}(r)=\sigma(r)^q[F^{+}(q)+F^{-}(q)] \tag{45}$$

for arbitrary q [cf. Eq. (39)]. Thus the Kolmogorov hypotheses are again recovered.

We see that

$$S_q^{\pm}(r)=\sigma(r)^q F^{\pm}(q). \tag{46}$$

Therefore, the ratio of positive and negative parts, analogous to Eq. (40), can be calculated,

$$\frac{S_q^{+}(r)}{S_q^{-}(r)}=\frac{F^{+}(q)}{F^{-}(q)}. \tag{47}$$

Note that there exist functions $P^{\pm}(y)$ that satisfy

$$\frac{F^{+}(q<1)}{F^{-}(q<1)}>1, \quad \frac{F^{+}(q>1)}{F^{-}(q>1)}<1, \quad \frac{F^{+}(1)}{F^{-}(1)}=1 \tag{48}$$

[cf. Eq. (43)]. This ensures that the experimental rule [6] is satisfied.

Up to this point, this asymmetric distribution works. However, it follows from Eq. (45) that, for $q=0$,

$$S_0^{\pm}(0)=0, \quad S_0^{\pm}(r>0)=F^{\pm}(0)=\text{const}, \tag{49}$$

in sharp contrast to the experiment: the functions are not at all constant; see Fig. 2. Moreover, as seen from Eq. (47), the ratio for any q is a constant, again in sharp contrast with direct measurements of these quantities (see Fig. 3 in [6]).

In spite of these apparent discrepancies with experiment, we will attempt to find theoretical possibilities for near-Gaussian distributions. Note first that there is no way to make the function $P(y)$ in Eq. (31) look Gaussian. If, say, we write

$$P(y)=\frac{1}{\sqrt{2\pi}\sigma(r)}\,e^{-(u-a)^2/2\sigma(r)^2}$$

in order to make it asymmetric, we find that $a=0$, due to requirement (43). But then, the PDF is symmetric. Therefore, we return to the pseudo-Gaussian form (37) and (41).

The distribution (37) and (41) seems to be physically feasible. We study therefore the two-point PDF, which would result in this kind of distribution. Recall that the Gaussian PDF for velocity increments (4) has been obtained from the two-point distribution (2), also Gaussian, of course. The latter can be naturally generalized to an asymmetric one to give Eqs. (37) and (41). Indeed, the distribution coincides with the Gaussian are with variance $\sigma^{+}(r)$ for $v>v'$ and with variance $\sigma^{-}(r)$ otherwise, namely,

$$P_2(u=v-v'>0,\,v'|r=x-x') = \frac{1-s}{d_2^{+}}\exp\left\{-\frac{u^2}{2\sigma^{+}(r)^2}-\frac{(v'+u/2)^2}{2[K(0)-\sigma^{+}(r)^2/4]}\right\} \tag{50a}$$

and

$$P_2(u=v-v'<0,v'|r=x-x') = \frac{1+s}{d_2^{-}}\exp\left\{-\frac{u^2}{2\sigma^{-}(r)^2}-\frac{(v'+u/2)^2}{2[K(0)-\sigma^{-}(r)^2/4]}\right\}, \tag{50b}$$

where $d_2^{\pm}=2\pi\sigma^{\pm}(r)[K(0)-\sigma^{\pm}(r)^2/4]^{1/2}$. If $r\to -r$, then these two distributions exchange because the whole PDF should be symmetric to the $v\to v'$, $x\to x'$ transformation.

Integrating Eq. (50) over all v', we indeed recover Eqs. (37) and (41). Now, if we integrate the two-point PDF over u, we should recover the one-point Gaussian distribution for v',

$$P_1(v')=\frac{1}{\sqrt{2\pi K(0)}}\,e^{-v'^2/2K(0)},$$

which indeed happens with the classical Gaussian distribution (2). But it is *not* the case for the quasi-Gaussian distribution (50). The integration results instead in

$$\frac{1}{\sqrt{2\pi K(0)}}\,M(v',r)e^{-v'^2/2K(0)},$$

where

$$M(v',r)=\frac{1}{\sqrt{2\pi}}\left\{(1+s)\int_{-\infty}^{z^-}e^{-x^2/2}dx+(1-s)\times\int_{z^+}^{\infty}e^{-x^2/2}dx\right\},$$

$$z^{\pm}=v'\,\frac{\sigma^{\pm}(r)}{2}\,\frac{1}{\{K(0)[K(0)-\sigma^{\pm}(r)^2/4]\}^{1/2}}.$$

Of course, for the symmetric distribution, $s=0$, $z^+=z^-$, and $M=1$. Asymmetry results in a one-point distribution depending on r and v', which does not make any sense at all. Thus the distribution (50) is not physically feasible.

VI. MEASUREMENTS OF THE PDF FOR THE VELOCITY INCREMENTS

The two-point PDF's are complicated to measure, but the PDF for the velocity increments is known relatively well; see, e.g., [14]. These studies show that, first, although the asymmetry is noticeable it is not very strong and, second, the PDF does not strongly deviate from the Gaussian form. This happens because the PDF is known well for small and moderate velocity increments. The intermittency effects are manifested mainly in the high-energy tails of the PDF; see [11], Sec. VII and Fig. 4 therein. But, in order to estimate the tails, one usually tries to measure high moments (the higher the better) and, as already mentioned in the Introduction, this is not easy to perform because of poor convergence.

The deviation from the one-parameter form was already seen from earlier experimental data [15]. The PDF is similar to Eq. (31), but with the additional function

$$P(u,r)\sim\frac{1}{\sigma(r)}\,e^{-|y|^{m(r)}}.$$

If m is a constant, then the PDF has one parameter. However, the PDF has actually two parameters because the second function $m(r)$ is involved. As claimed in [11], it is because of this function that the multifractal structure of turbulence becomes possible.

As mentioned, the experimental PDF does not strongly deviate from the Gaussian distribution for small and moderate velocity increments. Moreover, a more or less arbitrary, simple, and smooth function with a maximum at the origin can be fitted to a Gaussian distribution. The question is, however, if the latter corresponds to a two-point Gaussian distribution (1). As we saw in Sec. II, this would result in a one-parameter distribution for the velocity increments (4). We want to address an even more general question, that is, if any one-parameter functions for the velocity increments would fit the experimental data. In Sec. V some indirect evidence was presented suggesting that the answer is negative.

Figure 5 presents direct measurements of the PDF's. These are constructed in dimensionless form, that is, the (dimensionless) probability function $P(u/\sigma(r))$ is plotted against normalized increments $u/\sigma(r)$, where $\sigma(r)=\langle\Delta v_r^2\rangle^{1/2}$, and for different point separations r. If the distribution is Gaussian, then, according to Eq. (4),

$$P(u/\sigma(r))=P(y)=\frac{1}{\sqrt{2\pi}}\,e^{-y^2/2}. \tag{51}$$

Note that this function is independent of r and is depicted as a solid line in Figs. 5(a)–5(d). The experimental PDF's noticeably deviate from that curve. This deviation from the Gaussian form was already seen in Fig. 1 of Castaing, Gagne, and Hopfinger [14].

More generally, the PDF can be non-Gaussian, but with one parameter. In that case, it would be presented in the form (31), where $P(y)$ is some, generally asymmetric, function, but still independent of r. Figure 5 illustrates that the function $P(u/\sigma(r))$ definitely depends on r, which implies that the PDF is not a one-parameter function. One trend is indeed noticeable: the decreasing maximum of the PDF with increasing r, and, as a result, because of the normalization of the PDF, the increasing width with r. Only for substantially big separations do the curves collapse to one, as seen from Fig. 5(d) [16].

This trend is even more pronounced if we construct the distribution $P(u/{}^4\sigma(r))$, where ${}^4\sigma(r)=\langle\Delta v_r^4/3\rangle^{1/4}$; see Fig. 6 [for the Gaussian distribution $\sigma={}^4\sigma(r)$ because $\langle\Delta v_r^2\rangle^{1/2}=\langle\Delta v_r^4/3\rangle^{1/4}$].

In order to understand this trend and to make some quantitative statements, we note that, of course, each PDF in Figs. 5 and 6 can be fitted by a Gaussian distribution, although with variance $\sigma_2\neq 1$ and $\sigma_4\neq 1$, in contrast to Eq. (51). As a matter of fact, according to Figs. 5 and 6, this variance is a function of r and always $\sigma_2(r)<1$ and $\sigma_4<1$ because all experimental curves are narrower than the Gaussian one (51). An example of such a fitting is given in Fig. 7(a) for $r=1.27\eta$. We may call this pseudo-Gaussian fit because it does not correspond to the multivariate Gaussian process.

Now, why might the velocity increment $v(x+r)-v(x)$ statistics be expected to be Gaussian? Of course, if the velocity distribution is multi-Gaussian, then, as we saw in Sec. II, the PDF for $v(x+r)-v(x)$ would be Gaussian as well. More generally, if the one-point velocity distribution is Gaussian, then the increment for large separations r, presenting a sum of two independent processes $v(x+r)$ and $v(x)$, would be Gaussian as well. Figure 7(b) shows that experimental one-point velocity distribution deviates from the Gaussian one and again the PDF is narrower than the Gaussian one. This explains why the velocity increment PDF's for large distances still deviate from the Gaussian ones [Figs. 5(d) and 6(d)].

We return to the trend of increasing $\sigma_{2,4}$ with growing r. This can be understood if we suppose that the process is intermittent, implying that the PDF has high-energy tails; see, e.g., [11], Sec. VII B. Indeed, the PDF's in Figs. 5 and 6 cover the region up to three standard deviations, i.e., if the process is Gaussian, then that would cover 99.7% of events. Thus the tails give rise to higher probability of the events beyond 3σ, which corresponds to intermittency. It is known that the intermittency gives a relatively small impact in the inertial range, becoming more important as the scale r decreases and being maximal in a viscous range. This explains the trend in Figs. 5 and 6: the deviation from Gaussian distribution is more pronounced at small scales.

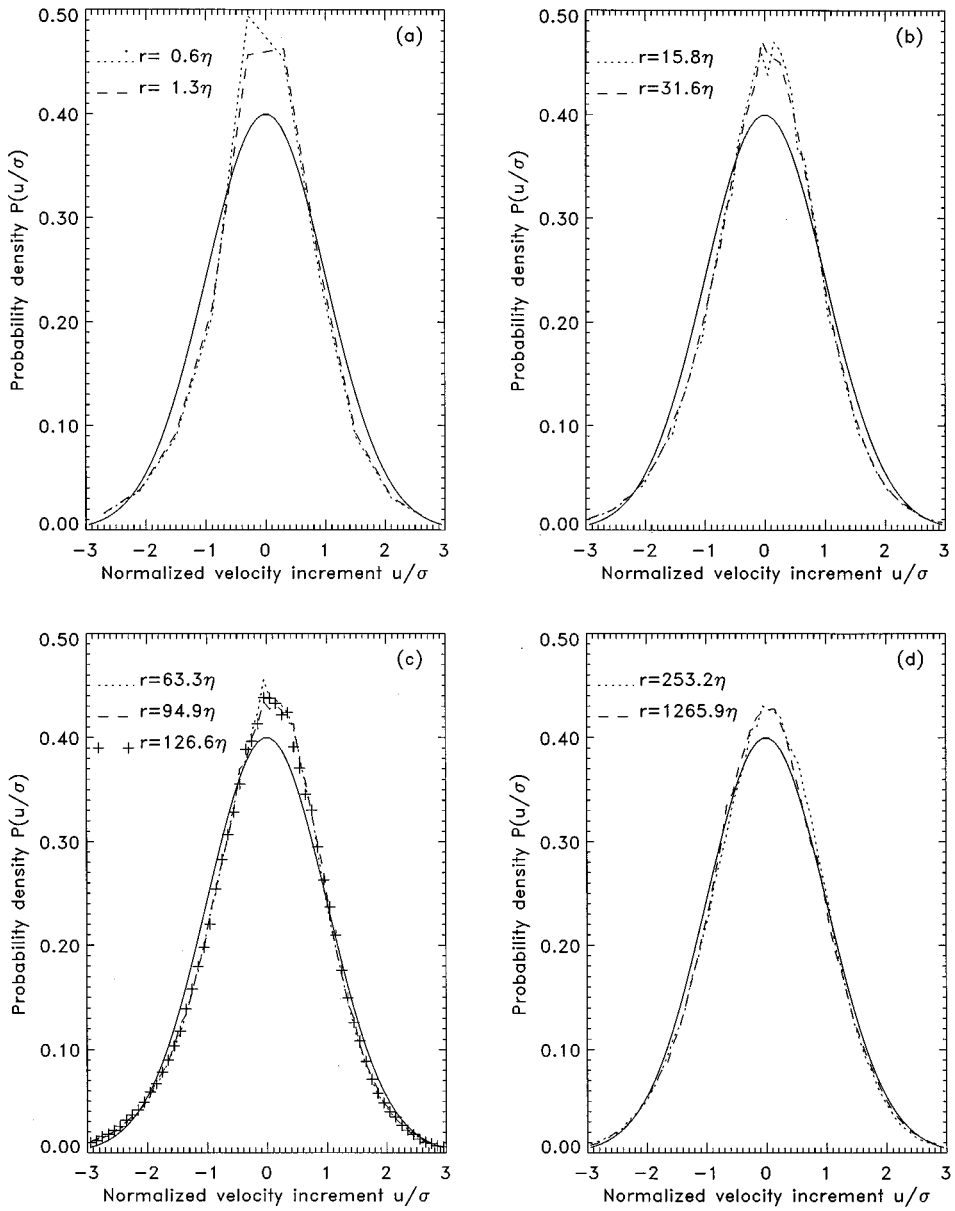

FIG. 5. Probability density $P(u/\sigma(r))$ for different point separations r. Here $u=\Delta v_r$ and $\sigma(r)=\langle \Delta v_r^2\rangle^{1/2}$. Each plot contains a Gaussian distribution, depicted with a solid line.

The trend itself is more noticeable in Fig. 6 because the PDF's are normalized through higher moments, that is, through the fourth moment, where the high-energy tails play a more important role. To be more specific, note that $\sigma_{2,4}(r)$ are defined as

$$\sigma_2(r)^2=\frac{\int_{-cr}^{cr} u^2P(u|r)du}{\langle \Delta v_r^2\rangle \int_{-cr}^{cr} P(u|r)du},$$

$$\sigma_4(r)^4=\frac{\int_{-cr}^{cr} u^4P(u|r)du}{\langle \Delta v_r^4\rangle \int_{-cr}^{cr} P(u|r)du}, \tag{52}$$

where $cr=3\sigma(r)$ and obviously $\sigma(r)^2=\int_{-\infty}^{\infty}u^2P(u|r)du$. The denominator can be written in the form

$$\int_{-cr}^{cr} P(u|r)du=1-\int_{-\infty}^{-cr} P(u|r)du-\int_{cr}^{\infty} P(u|r)du.$$

Considering corrections to unity in this expression to be small, we write Eq. (52) in a different way,

$$\sigma_{2,4}(r)^2=1-\int_{-\infty}^{-cr}\left(\frac{u^{2,4}}{\langle \Delta v_r^{2,4}\rangle}-1\right)P(u|r)du - \int_{cr}^{\infty}\left(\frac{u^{2,4}}{\langle \Delta v_r^{2,4}\rangle}-1\right)P(u|r)du. \tag{53}$$

The integrands in this expression are positive and therefore

$$\sigma_{2,4}(r)<1,$$

which is indeed observed; see Figs. 7(c) and 8. It is also obvious that the (negative) correction to unity in Eq. (53) increases with growing energy in the tails, that is, with grow-

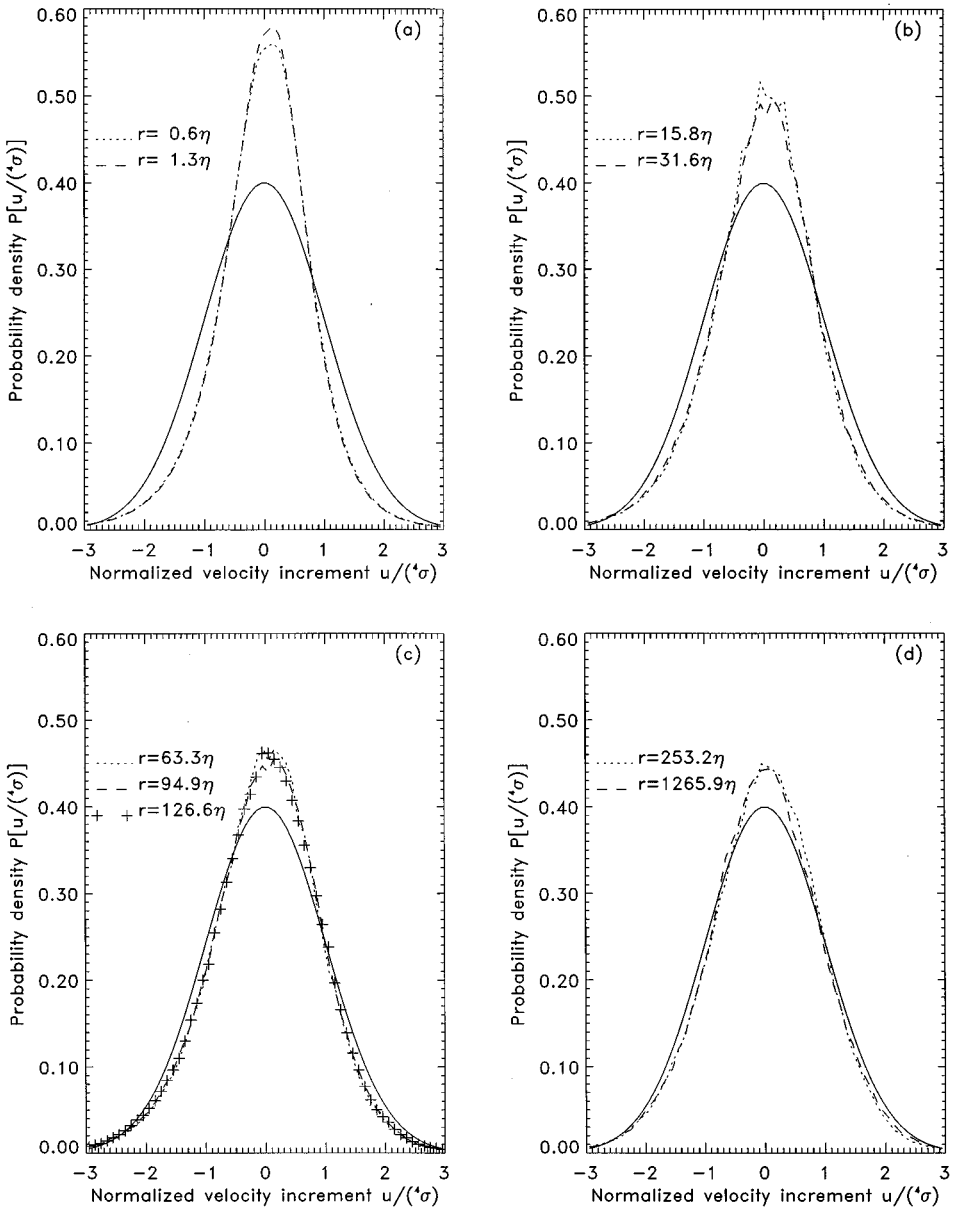

FIG. 6. Same as in Fig. 5, but with ${}^4\sigma(r)=\langle \Delta v_r^4/3\rangle^{1/4}$. Note that the trend of increasing width with growing r is more pronounced here than in Fig. 5.

ing $P(u|r)$ for $|u|>cr$. More specifically, if $P(u|r)$ for $|u|>cr=3\sigma(r)$ is (exponentially) small, then the correction would be negligible. Furthermore, for the Gaussian process or, generally, for any one-parameter PDF, this correction is independent of distance r (see Sec. V). From Figs. 5 and 6 we see, however, that the width is minimal (i.e., this correction is maximal) at small scales, where intermittency is expected to dominate.

As mentioned, the tails in the PDF are responsible for intermittency. Traditionally, this is described by the intermittency corrections to the Kolmogorov scaling, that is, the exponents ζ_q in Eq. (8) are given in the form

$$\zeta_q=\frac{q}{3}-\mu_q,$$

where μ_q are the intermittency correction; cf. Eq. (12). Note that $\mu_{q<3}<0$ and $\mu_{q>3}>0$. It follows from Eqs. (31) and (32) that all intermittency corrections μ_q vanish for the Gaussian distribution or, generally, for the one-parameter distribution (no tail). Therefore, we may try to interpret the scaling for $\sigma_{2,4}(r)^2$ as intermittency exponents. As a matter of fact, the scaling for these quantities, extending for more than two decades [Figs. 7(c) and 8], is better if compared with traditional measurements of the structure functions scaling: the latter is often presented only by somewhat more than one decade. It then follows from Figs. 7(c) and 8 that $\mu_2=-0.028\pm0.001$ ($\mu_2=-0.033$ from [4] and $\mu_2=-0.029$ according to [17]) and $\mu_4=0.086\pm0.003$ ($\mu_4=0.133$ from [4] and $\mu_4=0.054$ from [17]).

We see that the scalings for $\sigma_{2,4}(r)$ correspond to the intermittency exponents, obtained either from direct experimental measurements or from theoretical considerations: they are in between these two. In spite of that, this interpretation is not unambiguous because the analogy between $\sigma_{2,4}$ and the intermittency exponents is not straightforward. In any case, the r dependence of $\sigma_{2,4}(r)$ indicates a deviation from the Gaussian process or, more generally, from the one-

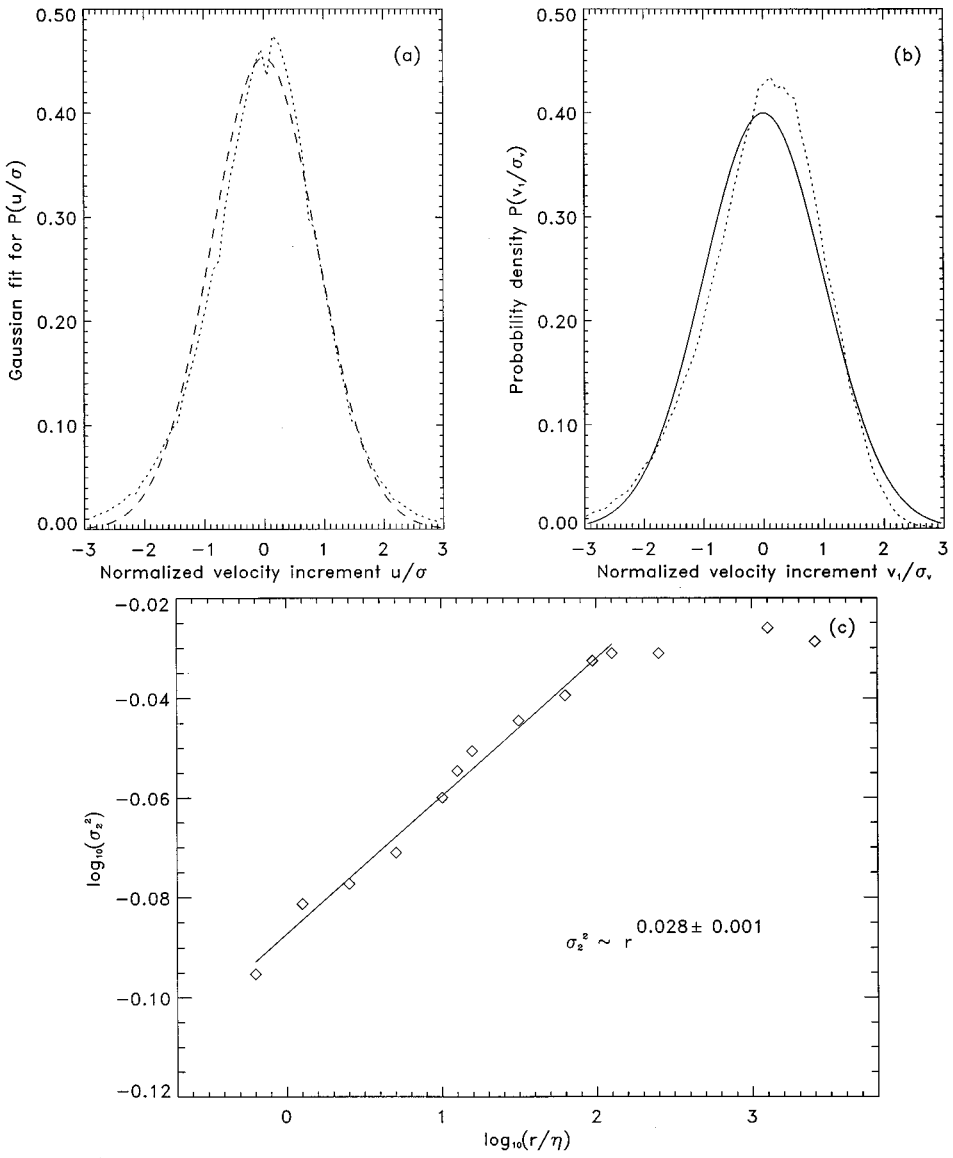

FIG. 7. (a) Pseudo-Gaussian fit (dashed line) for the PDF with $r=12.7\eta$ and $\sigma(r)=\langle \Delta v_r^2\rangle^{1/2}$. The PDF itself is depicted with a dotted line. (b) One-point velocity distribution (dotted line) $P(v_1/\sigma_v)$, with $v_1=v-\langle v\rangle$ and $\sigma_v=\langle v_1^2\rangle^{1/2}$, compared with the Gaussian (solid line). (c) Scaling for $\sigma_2(r)^2$, that is, the effective width of the PDF's. It follows that $\sigma_2(r)\sim r^{0.014}$, which confirms quantitatively the trend of the widening of the PDF with growing r.

parameter PDF. As mentioned above, this is an indication of intermittency, and the mere existence of the scaling, as seen from Figs. 7(c) and 8, suggests that the intermittency manifests itself in the inertial range.

VII. CONCLUSION

Although the measurements of high-order statistics provide direct evidence of intermittency, they have the disadvantage of being of poor convergence. On the other hand, low-order moments provide good statistics. Therefore, the study of the low-order statistics of positive and negative parts of the velocity increments might give some additional insight into the understanding of intermittency.

It was shown in Secs. III and IV that structure and correlation functions of zeroth order for positive and negative parts deviate from the Gaussian distribution. In particular, the box counting gives nontrivial Kolmogorov capacities for these parts separately.

Recall that traditionally, the asymmetry of turbulence is attributed to the energy cascade in fully developed turbulence [13]. It follows from the Navier-Stokes equation that the third moment does not vanish because it is responsible for the nonlinear interaction [3]; see Eq. (11).

Note that the asymmetry is supposed to be noticeable. Indeed, it is seen from the Kolmogorov law (11) that the third moment is not small, i.e., there is no physical, small parameter in the asymmetry. Indeed, one cannot claim that, e.g.,

$$|\langle [v(x+r)-v(x)]^3\rangle| \ll \langle |v(x+r)-v(x)|^3\rangle$$

because, according to the law (11), these quantities are of the same order of magnitude.

Thus the third moment is asymmetric. Recent studies revealed in addition that all moments, except for the first one, are asymmetric, in accordance with assumption (30), relating the asymmetry with intermittency [6].

We claim in this paper that the Kolmogorov hypotheses are equivalent to the assumption that the PDF for the velocity increments is a one-parameter function. Indeed, in Sec. II, the Kolmogorov scaling (12) and (13) is obtained from a

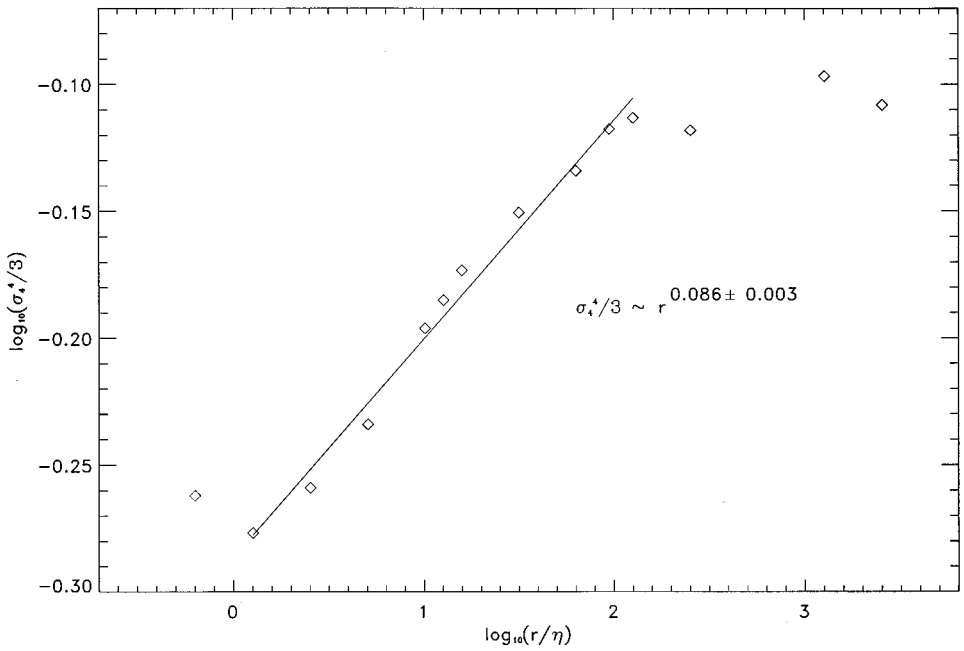

FIG. 8. Scaling for $\sigma_4(r)^4/3$. It is clear that $\sigma_4(r) \sim r^{0.022}$. Thus $\sigma_4(r)$ grows with r faster than $\sigma_2(r)$; cf. the caption to Fig. 7(c).

one-parameter (in particular, Gaussian) PDF. One the other hand, assuming Kolmogorov scaling, we recover the one-parameter PDF (31); see Sec. V. In other words, this type of PDF corresponds to nonintermittent turbulence.

In Sec. V we saw, however, that it is impossible to construct a Gaussian-like distribution of the one-parameter type (31) or in a slightly more complicated form (37) and (41). In addition, some evidence is given that, more generally, the one-parameter presentation of the PDF does not fit the experimental data and the quasi-two-parameter form (34) requires a jump in the PDF, which is never observed.

The experimental study of the PDF suggests that at least the two-point distribution deviates from the Gaussian form and, more generally, from the one-parameter function. The present study of the asymmetry gives additional evidence that the PDF is neither Gaussian nor of the one-parameter type. This in turn suggests that the simple Kolmogorov scaling (12) and (13) is modified by intermittency exponents. If we suppose that any functional changes in the inertial range can be presented as power laws, then the PDF for plus and minus distributions are presented as powers $\sim r^h dh$ and the exponents $\xi_q^{\pm}$ for the plus-minus distributions are obtained through the Legendre transform [11]. That returns us to the ramp model [9], with the main conclusion, namely, to inequality (30). The experimental study reported in this paper confirms this inequality.

ACKNOWLEDGMENTS

The measurements of the pipe turbulence were made at Yale University and were provided by K. R. Sreenivasan and R. Bhiladvala; I also appreciate discussions with them. I thank A. Yaglom, who suggested measuring the positive and negative parts of the velocity increments separately.

[1] A. N. Kolmogorov, C. R. (Dokl.) Acad. Sci. USSR **30**, 301 (1941).

[2] A. N. Kolmogorov, J. Fluid Mech. **13**, 82 (1962).

[3] A. N. Kolmogorov, C. R. (Dokl.) Acad. Sci. USSR **32**, 16 (1941).

[4] (a) F. Anselmet, Y. Gagne, E. J. Hopfinger, and R. A. Antonia, J. Fluid Mech. **140**, 63 (1984); (b) R. Benzi, L. Biferale, S. Ciliberto, R. Tripiccione, C. Baudet, F. Massaioli, and S. Succi, Phys. Rev. E **48**, R30 (1993); (c) G. Stolovitzky, K. R. Sreenivasan, and A. Juneja, *ibid.* **48**, R3217 (1993); (d) L. Zubair, Ph.D. thesis, Yale University, 1993 (unpublished).

[5] C. Meneveau and K. R. Sreenivasan, Nucl. Phys. B, Proc. Suppl. **2**, 49 (1987); R. R. Prasad, C. Meneveau, and K. R. Sreenivasan, Phys. Rev. Lett. **61**, 74 (1988); C. Meneveau, K. R. Sreenivasan, P. Kailasnath, and M. S. Fan, Phys. Rev. A **40**, 894 (1989); E. Aurell, U. Frisch, J. Lutsko, and M. Vergassola, J. Fluid Mech. **238**, 467 (1992); M. Borgas, Philos. Trans. R. Soc. London, Ser. A **342**, 379 (1993).

[6] K. R. Sreenivasan, S. I. Vainshtein, R. Bhiladvala, I. San Gil, S. Chen, and N. Cao, Phys. Rev. Lett. **77**, 1488 (1996); N. Cao, S. Chen, and K. R. Sreenivasan, *ibid.* **77**, 3799 (1996).

[7] C. Meneveau and K. R. Sreenivasan, J. Fluid Mech. **224**, 429 (1991).

[8] R. Benzi, S. Ciliberto, R. Tripiccione, C. Baudet, F. Massaioli, and S. Succi, Phys. Rev. E **48**, R29 (1993); G. Stolovitzky, K. R. Sreenivasan, and A. Juneja, *ibid.* **48**, R33 (1993).

[9] S. I. Vainshtein and K. R. Sreenivasan, Phys. Rev. Lett. **73**, 3085 (1994).

[10] H. G. E. Hentschel and I. Procaccia, Physica D **8**, 435 (1983); U. Frisch and G. Parisi, in *Turbulence and Predictability in*

Geophysical Fluid Dynamics, edited by M. Gil, R. Benzi, and G. Parisi (North-Holland, Amsterdam, 1985), pp. 84–88; G. Paladin and A. Vulpiani, Phys. Rep. **156**, 147 (1987).

[11] S. I. Vainshtein, K. R. Sreenivasan, R. T. Pierrehumbert, V. Kashyap, and A. Juneja, Phys. Rev. E **50**, 1823 (1994).

[12] Note that one-parameter PDF, like Eq. (31), in the framework of so-called extended self-similarity (ESS), would result in something similar to the Kolmogorov hypotheses, *for any* $\sigma(r)$, even without any scaling whatsoever. Indeed, it follows from Eq. (32) that $\log S_q(r) \sim q \log\sigma(r)$ and therefore $\log S_q(r) \sim (q/3)\log S_3(r)$. So, for one-parameter PDF, in particular, Gaussian, if $\log S_q(r)$ is plotted against $\log S_3(r)$, then the plots will look like as if Eq. (12) is satisfied, although the structure functions $S_q(r)$ might not have any scaling at all. Essentially, one-parameter PDF means a nonintermittent process. We might expect that this could be violated at small r's, where the intermittency is more pronounced. Nevertheless, the ESS still holds for small r, for real turbulence. The point here is that due to the analytical nature of the process, we have $S_q(r) = a_q r^q$ for small r. Here a_q are some constants, so that, say, the flatness, which is equal to a_4/a_2^2, by Eq. (15), could be big. Nevertheless, since expression $S_q(r) = a_q r^q$ has the form of Eq. (32), the ESS does hold, that is, again $\log S_q(r) \sim (q/3)\log S_3(r)$ in spite of the fact that $S_3(r) \sim r^3$ in this range.

[13] A. S. Monin and A. M. Yaglom, *Statistical Fluid Mechanics* (MIT Press, Cambridge, MA, 1971), Vol. 2.

[14] B. Castaing, Y. Gagne, and E. J. Hopfinger, Physica D **46**, 177 (1990); R. Benzi, L. Biferale, G. Paladin, A. Vulpiani, and M. Vergassola, Phys. Rev. Lett. **67**, 2299 (1991); A. Noullez, G. Wallace, W. Lempert, R. B. Miles, and U. Frisch, J. Fluid Mech. (to be published).

[15] P. Kailasnath, K. R. Sreenivasan, and G. Stolovitzky, Phys. Rev. Lett. **68**, 2766 (1992).

[16] This trend was also noticed in the PDF measured in helium gas turbulence; see P. Tabeling, G. Zocchi, F. Belin, J. Maurer, and H. Willaime, Phys. Rev. E **53**, 1613 (1996). The PDF is plotted on a linear-logarithmic scale and, as the authors note, ''[the] tip appears as parabolic with a radius of curvature decreasing as the scale is decreased.'' Recently, B. Dhruva and K. R. Sreenivasan (private communication) observed this trend from atmospheric turbulence measurements, with the Taylor microscale Reynolds number $R_\lambda = 9540$.

[17] Z.-S. She and E. Leveque, Phys. Rev. Lett. **72**, 336 (1994).